POAC '99
Espoo, Finland

Proceedings of the 15th
International Conference on
Port and Ocean Engineering
under Arctic Conditions

ICE FORCE DISTRIBUTION AROUND A SHIP HULL

Koh Izumiyama, Daisuke Wako and Shotaro Uto
Ship Research Institute, Japan

ABSTRACT

Resistance tests were performed at the ice tank of Ship Research Institute of Japan for a model of the *PM Teshio*, an ice-breaking patrol ship of the Maritime Safety Agency of Japan. A new type of pressure sensor was used in the test to measure local ice loads acting on the model hull. With the sensor it is possible to make pressure measurements with a very high spacial resolution of 5.4 mm. Local ice loads were measured along the waterline of the model at the bow from the stem to station No. 6-1/2. It was shown that the hull-ice contact takes place in narrow line-like areas. Discussion will be made on the vertical and horizontal distributions of local ice loads.

1. INTRODUCTION

Ice loads acting on a ship can be treated in two ways; global and local. The lateral component of the global ice load appears as ship resistance that governs ship's performance in ice. Hull form, especially bow form, has to be designed so that the ship can achieve required performance in ice under a given propulsive power. Model testing at an ice tank is an indispensable procedure for the design of ice-going ships today. Model ships are towed in ice of scaled mechanical properties. Main objective of the model testing is to estimate ice resistance and power required in given conditions.

The global ice load is an integrated value of local loads over the hull area. The magnitude and distribution of local ice loads at model testing, therefore, have to be properly scaled from those at full-scale. There have been, however, very little studies done to evaluate the local ice loads at model scale. One of such studies was made by Liukkonen et al (Liukkonen et al, 1992). They performed resistance tests at an ice tank using a segmented model to measure local ice loads acting on each segment. Their study showed that ice load is dominant at the bow of the model. Segments of their model, however, were not small enough to see detailed behaviour of local ice loads.

Recently, a new type of pressure sensing system, called the tactile sensor, is used in testings in ice. The sensing system is composed of sensor films and a computer. On the sensor film there are about 2,000 pressure sensing spots in a grid-like arrangement. With this sensor system pressure measurements of a very high spacial resolution can be achieved. Izumiyama et al. (1998) made a first attempt to use the sensor in an indentation test in ice tank to measure ice pressure distribution against a flat indentor. Sodhi et al. (1999) used the sensor in a field indentation test at the Notori lagoon in Japan. In these studies the sensor system was successful to show ice-indentor contact and ice load distribution on the indentors. It was shown that the sensor is a useful tool for tests in ice both in laboratory and field.

In this study it was attempted to use the tactile sensor for a model testing of a ship to measure local ice load on the model hull. Objectives of this study are; to check the applicability of the tactile sensor to the ship testing, to study the ice loading scenario, and to study ice load distribution around the hull. Resistance tests were performed at the ice tank of Ship Research Institute, Japan for a model of ice-breaking patrol ship. Ice load measurements by the tactile sensor were made at six different locations of the model bow along the waterline from the stem to the station No. 6-1/2. This paper presents methods and results of the test.

2. MODEL TEST

2.1 Model Ship and Testing Apparatus

Resistance tests were performed at the ice tank of the Ship Research Institute. The tank is 35 m in length, 6 m in width and 1.8 m deep. Model ice doped with Propylen Glycol (PG-ice) was used for the test.

A model of the *PM Teshio*, an ice-breaking patrol ship of the Maritime Safety Agency of Japan, was used for the test. Table 1 summarizes the principal dimensions of the ship and model. The scale of the model was 1:10.89. Tests were made for ship draft of 3.30 m, which is 0.303 m in the model.

Figure 1 shows a schematic of the experimental setup. The model was connected to the towing carriage via a towing post and guiding post. The guiding post is free to surge. The model was free to pitch, heave and roll. Total resistance of the model was measured by a dynamometer placed between the towing post and the model. Motions of the model were measured by potentiometers installed on the model. The measured data were stored on a data recorder. A real time analysis of the data was also performed using a desk-top computer on the carriage.

Table 1 Principle Dimensions

	Ship	Model
Length Overall,	55.0	5.051
Molded Breadth, m	10.6	0.973
Draft, m	3.3	0.303

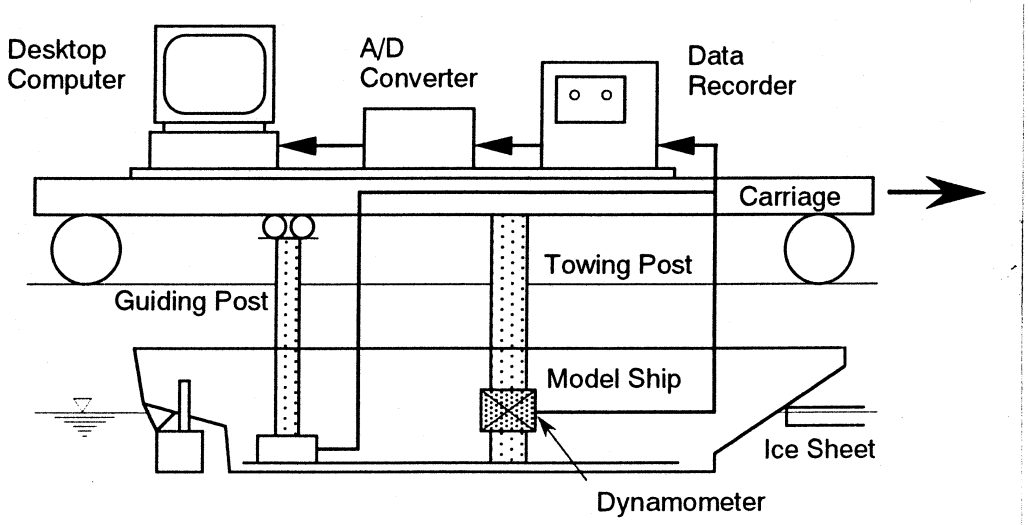

Figure 1 Experimental Set-up

2.2 Pressure Sensing System

A tactile sensing system was used to measure pressure acting on the model hull. Details of the sensing system is given by Izumiyama et al (1998). The system is composed of two pressure sensors and a computer to acquire, process and store the data measured at sensors. The sensor is a thin (about 0.3 mm thick) and flexible film of a size of 240 mm by 240 mm. On the film there are sensing spots in a grid-like arrangement of 44 rows by 44 columns. Spacing between sensing spots is about 5.4 mm.

Pressure changes at each grid point on the sensor film are converted into voltage change and acquired by the computer. Data from the sensor films are treated as 8-bit data, called raw data, in the computer. The computer creates a data set which contains pressure readings at grid points over the entire area of the film, called a frame. Pressure distribution is displayed by a computer monitor. Not only the real-time monitoring of data, the system has a function to record measured data as a computer file. Data can be recorded at a sampling frequency up to 100 frames per second. The data files can also be converted into ASCII files so that they can be further analyzed by other softwares or programs. The system also has a function to calculate the sum of raw data, called a raw sum, at sensing spots within any desired rectangular area in a pressure film.

Nominal measuring capacity of the pressure film used in this study is 200 kPa. Raw data of 256, therefore, would correspond to the pressure of 200 kPa on a sensing spot. Izumiyama et al. (1998), however, showed non-linearity between the load applied to a sensor film and the raw sum given by the system. They also discussed that the raw data depend not only on the pressure but also loading area within a sensing spot. In this paper, taking these facts into account, results measured by the tactile sensor will be given as forms of raw data or raw sum. They will not be converted to pressure or load. Despite of the calibration problems, the sensor is a very useful tool, because it gives data on actual ice-hull contact area or comparative ice pressure with a very high spacial resolution that has never been achieved by other devices.

2.3 Test Scheme

Sensor films were pasted on the model hull at the waterline. Figure 2 shows the locations of the sensor films on the model. Ice pressure on the model hull was measured at six different locations so that they covered the ship bow up to from F.P. to the station 6-1/2. Since the tactile sensor system used for this test can handle two sensor films, three tests were performed for same conditions with different sensor locations. Figure 3 is a photograph of pressure sensors pasted at locations No. 1 and 2.

Tests were performed for ice thickness of 41 mm, which is 45 cm at full-scale, and for level ice and broken ice conditions. In level ice sheet two tests were performed at different model speeds of 0.156 m/s and 0.779 m/s, which were 1 and 5 knots at full-scale, respectively. After the tests ice was manually broken to form a broken ice field. Another test was then performed in the broken ice at 1.559 m/s which is 10 knots at full-scale. Elasticity and flexural strength of ice were measured before the model runs by way of the plate deflection method and bending tests of cantilever beams cut in the ice sheet, respectively.

Table 2 summarizes tests conditions. Local ice loads in broken ice field were considerably low compared with those in level ice. In this paper results of tests in level ice will be presented. Data from the tactile sensor was not available for tests No. 1 and 2 due to malfunction of the sensor system.

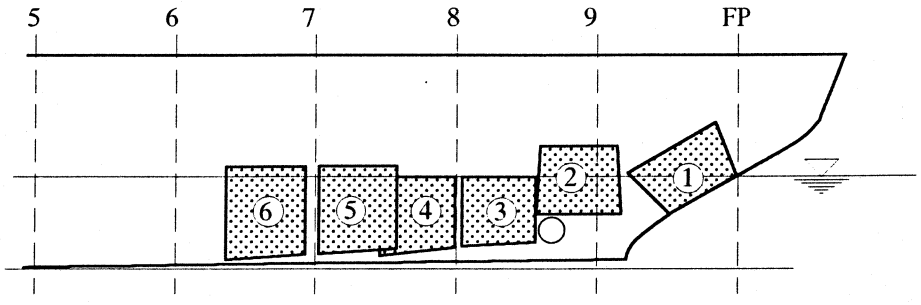

Figure 2 Locations of Sensor Films

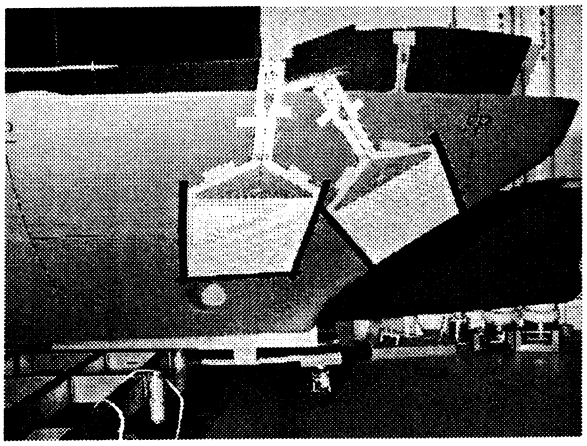

Figure 3 Photograph of Sensor Films on the Model

Table 2 Summary of Test Conditions

Test No.	Sensor Locations	Model Speed, m/s	Ice Thickness, mm	Ice Condition
1	1,2	0.156	41.3	Level
2	1,2	0.779	41.3	Level
3	1,2	1.559	41.3	Broken
4	3,4	0.156	42.5	Level
5	3,4	0.779	42.6	Level
6	3,4	1.559	42.6	Broken
7	5,6	0.156	42.2	Level
8	5,6	0.779	42.5	Level
9	5,6	1.559	42.4	Broken

3. RESULTS AND DISCUSSION

3.1 Ice-hull Contact

Figure 4 is an example of data obtained by the tactile sensor system. The figure shows a typical pattern of model-ice contact in level ice at model speed of 0.779 m/s. Figures 4 (a)-(g) are frames which show pressure distribution on a sensor film at location No. 3. The waterline of the model is at the top of the frames and the left side of the frames is the bow side. Figure 4 (h) is a time trace of raw sum of data over the film. The figure shows data for a time period of 0.7 second.

The process shown in Figure 4 is composed of two different phases in terms of ice-model contact and ice load. The first phase lasts from time of 0.05 to 0.5 seconds in Figure 4 (h). Four frames during this phase are shown in Figures 4 (a)-(d). The second phase takes place after the time of 0.5 second, and three frames are shown in Figures 4 (e)-(g) for this phase. In the first phase it is seen that relatively high pressure is acting over narrow area as shown in Figures 4 (a)-(d). The pressured areas are distributed so that they form a line. The line moves downwards and disappears at time of 0.5. The total load acting on the sensor shows a peak at time of about 0.2 second. In the second phase relatively low pressure acts in the wider area. The pressured area moves upwards in this phase. The total load shows another peak at time of 0.6 second.

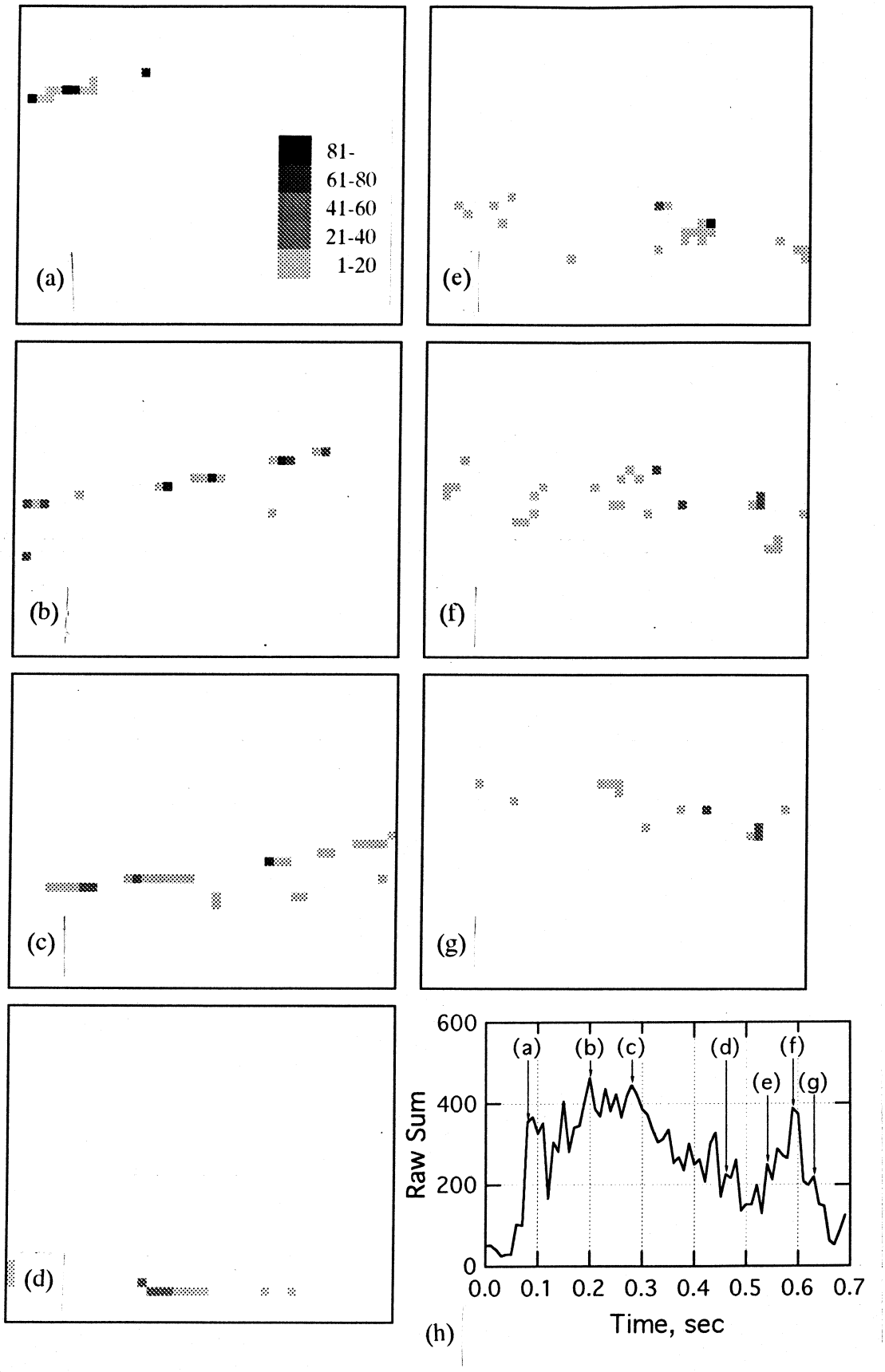

Figure 4 Example of Measured Ice Load

Riska et al carried out a field test on board the icebreaker *Sampo* in which they measured ice load distribution acting on the ship hull by using a PVDF-plate (Riska et al, 1990). They also installed a lexan window in the hull to make a direct observation of ice-hull contact. Their measurements and observations showed that the ice-hull contact takes place over narrow line-like areas. The pressure distributions shown in Figures 4 (a)-(d) also show that the ice pressure acts in a narrow line-like area. The line is of width of one sensing spot in most cases. Since the spacing between sensing spots is 5.4 mm, the lines are significantly narrow compared with full thickness of ice that is 41 mm. It should be noted that 5.4 mm is the highest spacial resolution for the sensor films used in this test. Actual contact area therefore can be narrower than this. It is now shown that the line-like contact which was observed by the field test also takes place in the model test.

As shown in Figures 4 (e)-(g) loading in the second phase is completely different from that in the first phase. This type of hull loading was not reported by Riska et al. Mechanism that causes this loading is not known. There are, however, several facts that can help to consider this loading scenario. Firstly, this type of loading was in most cases preceded by the line-like contacts as in the first phase shown in Figure 4. Secondly, this type of loading was obtained only in the tests at model speed of 0.779 m/s and was not seen in the tests at model speed of 0.156 m/s. From these facts it is likely that this type of loading was caused by the rotation of ice pieces after the breaking of ice. Figure 5 schematically shows the loading scenario. Ship hull contacts the edge of an intact ice sheet (Figure 5 (a)), and the ice is pushed down as the ship advances (Figure 5 (b)). During this phase line-like contact takes place. The ice breaks (Figure 5 (c)), and, by being pushed by incoming new edge of ice, the broken ice piece rotates toward the ship hull (Figure 5 (b)). If ship speed is high enough, and so is the rotation speed of the broken ice piece, this process can cause loading on the ship hull. Hydrodynamic force will mainly attribute to the loading in this phase. Hydrodynamic loading results in relatively low pressure and wider pressured area than that by direct contact with ice. Loading scenario due to the rotation of ice piece will also explain the fact that the loaded area moves upwards.

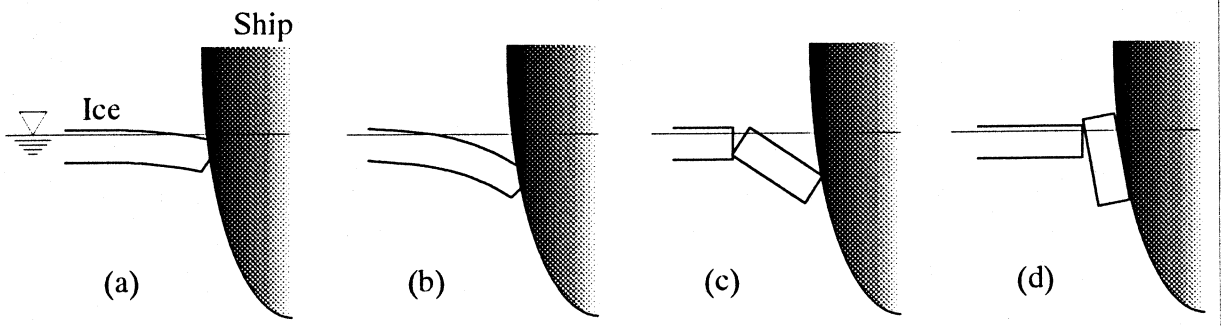

Figure 5 Loading Scenario

3.2 Ice Load Distribution

Ice-going ships are armoured with thick shell platings to resist ice loads. Especially, it is a common design practice to thicken shell plating along the waterline to form what is called an "ice-belt". Length and height of the ice-belt should be determined so that it covers the area of hull that is exerted by high ice loads. In this study three sets of resistance tests were repeated for same conditions but with different locations of pressure films. Ice load distribution at different hull areas can be obtained by comparing these tests.

Figure 4 shows that the ice-hull contact takes place in a narrow line-like area, and the area moves downwards as the ship advances. For the design of the ice-belt it will be useful to

know the vertical distribution of ice load beneath the waterline. To calculate the vertical distribution of ice load from the data measured by pressure films, eleven sub-areas are selected on the film as shown in Figure 6 (a). Each sub-area is of 22 mm high and 86 mm wide composing 4*16 sensing spots, and are located at different elevations. Total load on each sub-area was calculated by summing up readings at all the sensing spots over the sub-area. Load levels of non-exceedance probabilities of 99, 98 and 95 % are calculated to represent peak load levels.

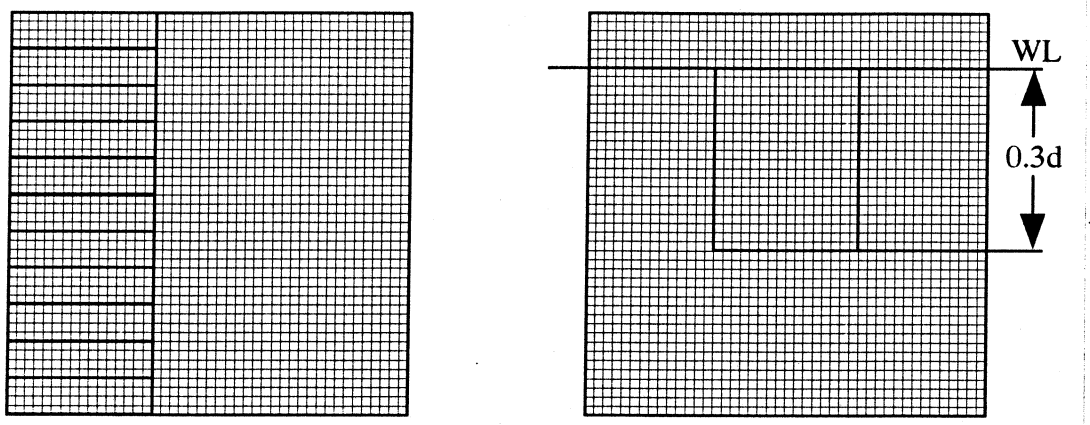

Figure 6 Sub-Areas for Analysis

Figure 7 shows vertical distribution of ice load in level ice at several different stations. Data at the station 9 is not available for the model speed of 0.156 m/s due to malfunction of the sensor system. There are several things to note in Figure 7. The figure shows that ice load is dominant over the area beneath the waterline up to the depth of about 30 % of ship draft. This depth is about 1 m beneath the waterline at full-scale. As a general trend peak ice load increases toward the shoulder of the ship. It is very interesting to note that there is no significant difference between the results at model speeds of 0.156 and 0.779 m/s in terms of peak ice load on the hull. At station 6-8/10 the peak load is even higher for the lower speed.

Besides vertical distribution, information on the horizontal distribution of ice load on the hull is also important. To analyze horizontal distribution of ice load sub-areas are selected on the sensor film. Each sub-area is of 86 mm wide and vertically covers an area between the waterline and the depth of 30 % ship draft where ice loading is dominant (Figure 6 (b)). Raw sum was calculated for each sub-area.

Figure 8 shows horizontal distribution of local ice load along the waterline. The distribution is relatively flat for the model speed of 0.779 m/s, while it varies along the waterline for the speed of 0.156 m/s. This may attribute to difference in cracking pattern of ice sheet for the two model speeds. At the higher speed ice sheet broke into smaller pieces than those at the lower speed. This can result in relatively even chance of ice-hull contact along the waterline. When the ice breaks into larger pieces, spacially biased contacts can take place. More data is needed, however, to confirm this hypothesis.

Time average ice load is important form a view point of ship resistance. Figure 9 shows distribution of average ice load along the waterline. As is naturally expected, model received larger load at the higher speed as shown in Figure 9. Difference of ice load between the two model speeds is significant in the area forward of station No. 7. Ice load measured by the pressure sensor is the normal load to the hull. Resistance can be calculated from the normal load by taking into account the ice friction coefficient and inclination angle of the hull. Information as shown in Figure 9 will be useful to the design of bow form of low ice resistance.

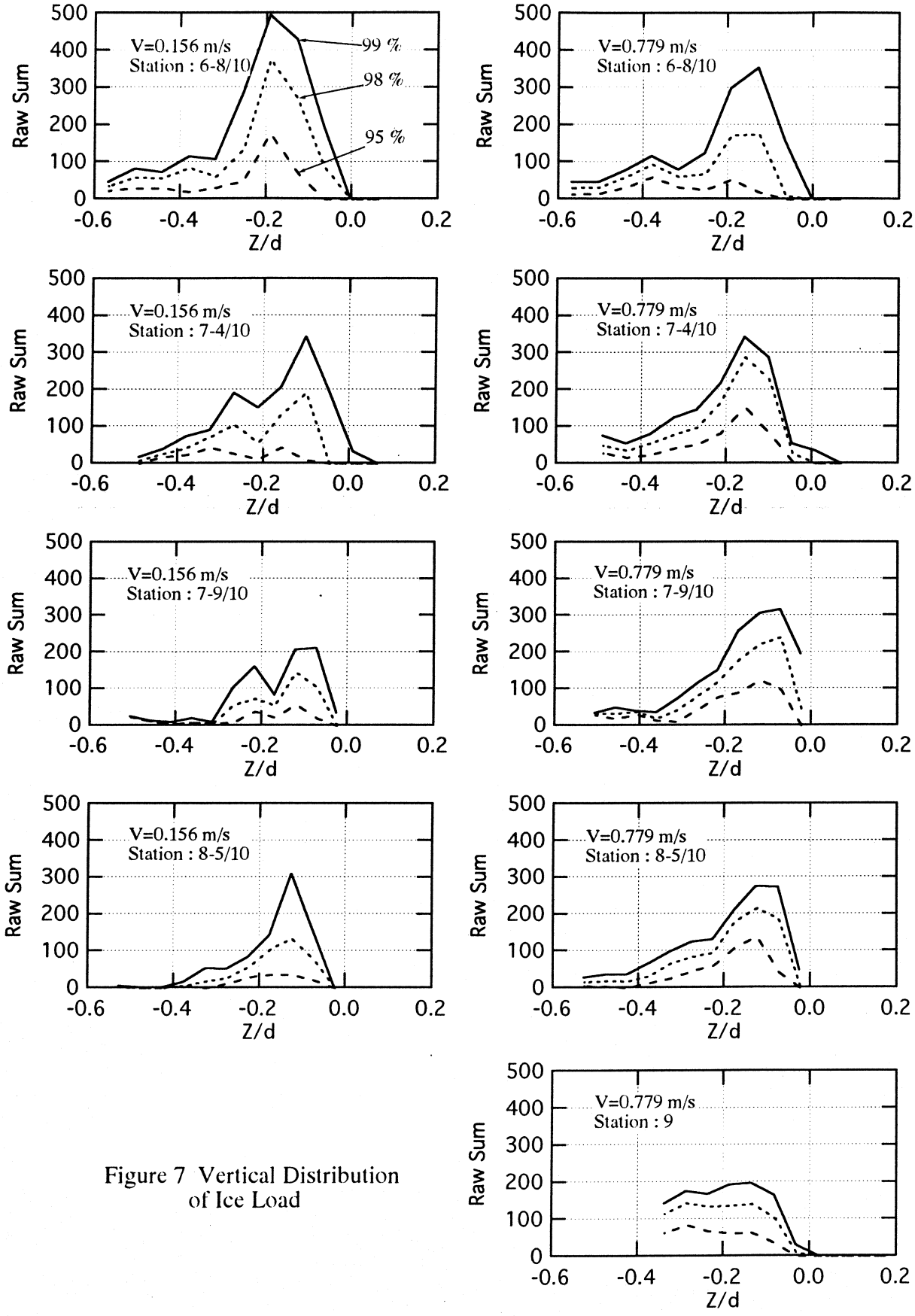

Figure 7 Vertical Distribution of Ice Load

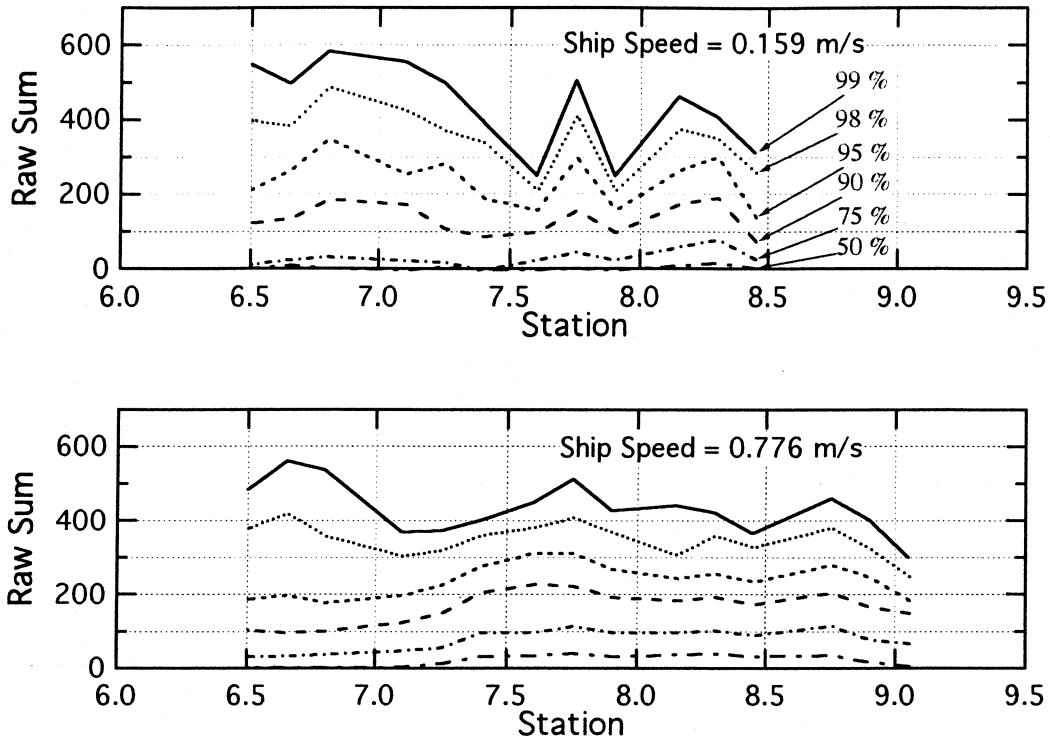

Figure 8 Horizontal Distribution of Ice Load

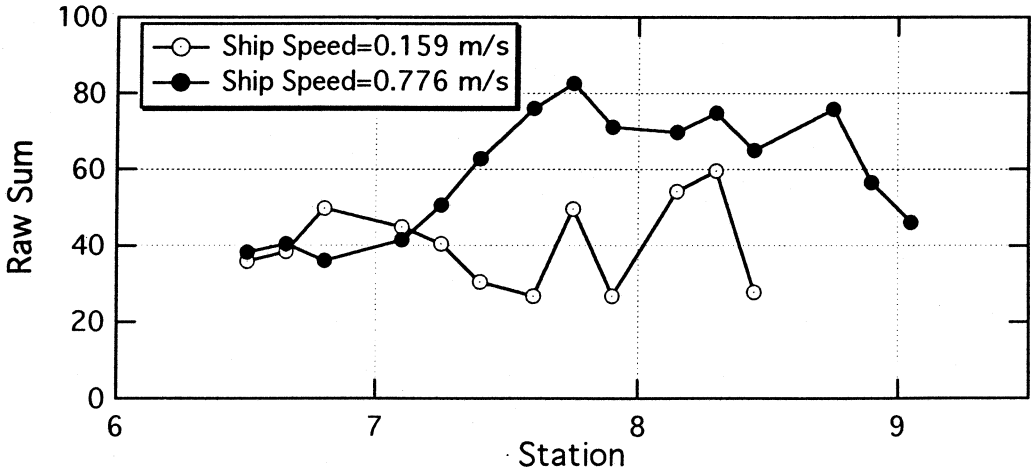

Figure 9 Horizontal Distribution of Average Ice Load

SUMMARY

This paper presented results of model experiment to study ice load distribution around a ship hull. Resistance tests were performed at the ice tank of Ship Research Institute, Japan using a model of the *PM Teshio*, an ice-breaking patrol ship for the Maritime Safety Agency of Japan. A pressure sensing system was used to measure ice pressure acting on the model. The pressure sensor gave data on ice contact area and ice pressure on the model hull with a very high spacial resolution of 5.4 mm.

In this paper results of model tests in level ice were presented. In level ice tests were performed for two different model speeds of 0.156 m/s, which is 1 knot at full-scale, and 0.779 m/s, 5 knots. Followings are summaries of this paper.

- It was shown that ice-hull contact takes place at a narrow line-like area as was observed in field tests.
- Different type of loading was also observed at the higher speed. This loading will be hydrodynamic force due to the rotation of broken ice pieces.
- Local ice load is dominant on the hull area between the waterline and the depth of about 30 % of ship draft, which is about 1 m beneath the waterline at full-scale.
- In terms of peak value of local ice load, there is no significant difference between the lower and higher model speed.
- In terms of time average ice load, the higher model speed gave the higher load. The difference is large in the area forward of station No. 7.

This model test was the first attempt to use the tactile sensor for ship test. Results of the test showed that the tactile sensor is successful to measure local ice loads on the model hull. Information on the distribution of local ice loads around the ship hull can be used for more effective design of ice-going ships both in terms of performance and structural points of view. Results presented in this paper are of the first stage of the research. It is planned to make further analysis and model testings on local ice loads.

REFERENCES

Izumiyama, K, Wako, D. and Uto, S., 1998. .Ice Force Distribution on a Flat Indentor. IAHR Ice Symposium, 1998.

Riska, K., Rantala, H. and Joensuu, A., 1990. Full Scal Observations of Ship-Ice Contact. Helsinki University of Technology., Otaniemi, 1990-02-12.

Sodhi, D.S., Takeuchi, T. and Nakazawa, N., 1999. Ductile to Brittle Transition Speed during Ice Indentation Tests. Proc. of REIFS, February 2-4, 1999, Mombetsu, Japan, pp.

Luikkonen, S. and Nortala-Hoikkanen, A., 1992. Ice Resistance Tests on a Segmented Icebreaker Model. Proc. of IAHR Ice Symp. 1992, vol. 1, pp. 296 - 306.